

Phase behavior of a binary symmetric mixture in slitlike pores with opposing walls: Application of density functional approach

Andrzej Patrykiewicz,^{1,*} Orest Pizio,^{2,†} Stefan Sokołowski,^{1,‡} and Zofia Sokołowska^{3,§}

¹*Department for the Modelling of Physico-Chemical Processes, Maria Curie-Skłodowska University, 20031 Lublin, Poland*

²*Institute of Chemistry, UNAM, Circuito Exterior, Coyoacan 04510, Mexico Distrito Federal, Mexico*

³*Institute of Agrophysics, Polish Academy of Sciences, Doświadczalna 4, 20290 Lublin, Poland*

(Received 25 July 2003; revised manuscript received 17 February 2004; published 4 June 2004)

We study adsorption of a symmetric binary Lennard-Jones mixture, which exhibits partial mixing in a bulk phase, in slitlike pores formed by the walls having antisymmetric properties with respect to the components. The calculations are carried out by means of a density functional approach. We show that under suitable conditions the pore filling may occur as a sequence of two first-order transitions. The capillary condensation may lead to an “antisymmetric” liquidlike film, the symmetry of which follows the symmetry of the adsorbing potential, or to a “demixed” film, the symmetry of which is only weakly associated with the symmetry of the adsorption potential. The additional first-order antisymmetric-demixed film transition begins at the triple point temperature and ends at the critical end point temperature.

DOI: 10.1103/PhysRevE.69.061605

PACS number(s): 68.08.De, 68.03.-g, 64.70.Fx

I. Introduction

The thermodynamic behavior of confined fluids significantly differs from that of a bulk fluid under identical thermodynamic conditions. The effects of confinement on phase transitions have been studied for a long time, cf. the review papers [1–4]. One of the most often explored pore models used for that purpose is a slitlike pore with energetically homogeneous walls. Such pores, if formed by two parallel infinite planes, are usually assumed to have the walls of identical adsorbing properties. The last assumption is not necessary and, in fact, the pore walls can exhibit different adsorbing properties. Several papers [4–12] have been published in the literature concerning the phase behavior of lattice models, including ferromagnetic Ising films, binary mixtures, and polymers confined to slitlike pores with the walls exerting opposing surface fields (the so-called “competing” or “opposing” walls). In such cases a novel type of phase transition can be observed. This transition occurs from a state of the fluctuating interface to a state of the localized interface, and is called the localization-delocalization transition. More detailed discussion of that problem can be found in a recent review paper [4].

Identical and competing walls are the two limiting cases of a more general situation in which the properties of both walls can be arbitrary. Therefore, it is of interest to investigate the pore models in which the adsorbing properties of the walls change from identical to opposing. In our recent papers we have investigated the adsorption of single-component fluids in slitlike pores with differently adsorbing walls [13,14]. Using lattice as well as off-lattice models we have observed that when the adsorption energy due to one wall is gradually

weakened, a single coexistence envelope, which describes capillary condensation in a pore with two identical walls, splits into several, layeringlike branches. “Dryness” at weakly attractive (or repulsive) wall “pushes” the adsorbate molecules towards the second, strongly adsorbing wall and enforces their clustering and thus facilitates the layering-type phase transitions.

The goal of this work is to extend our previous studies to the case of a binary mixture, exhibiting partial mixing in the bulk. The tool we use for that purpose is the fundamental measure of density functional approach [15,16], which we have recently applied to investigate adsorption of mixtures in pores as well as at single flat walls [17–21]. Similarly as in the works quoted above, we use a simple model of a binary mixture, which in the literature is known as a symmetric binary mixture [22–29]. The model involves two species, $j = 1, 2$, of equal diameters, $\sigma_1 = \sigma_2 = \sigma$, i.e., it ignores the influence of the size ratio on the phase behavior. Moreover, additivity of diameters is assumed and hence $\sigma_{12} = \sigma$. The interactions between like particles are assumed to be represented by identical functional form (Lennard-Jones potential) and are characterized by the same energy parameters, $\epsilon_{11} = \epsilon_{22} = \epsilon$. The “cross” interaction between unlike particles is also represented by the Lennard-Jones potential and characterized by the energy parameter $\epsilon_{12} < \epsilon$. It is worth mentioning that this model was widely applied to study adsorption [17–29] on solids, as well as to study an interface between two demixing fluids [30–33].

Obviously, this model, as well as the model of the fluid-pore interactions described below, are idealizations, in comparison to adsorbing systems in nature. However, the focus of our work is to reveal some general trends of the phase behavior of confined mixtures, and therefore we reduce the number of the model parameters to a minimum.

II. Theory

We assume that the pore walls are energetically homogeneous, so that the potential exerted by a single wall, $i = 1, 2$,

*Email address: andrzej@pluto.umcs.lublin.pl

†Email address: pizio@servidor.unam.mx

‡Email address: stefan@zool.umcs.lublin.pl

§Email address: zosia@maja.ipan.lublin.pl

$v_j^{(i)}(z)$ on the component j , is a function of the normal distance z only. The external field acting on a particle of j th kind, due to both pore walls, is given by

$$v_j(z) = v_j^1(z) + v_j^2(H - z), \quad (1)$$

where H is the pore width. We model the functions $v_j^i(z)$ by Lennard-Jones (9,3) potential

$$v_j^i(x) = \begin{cases} \varepsilon_j^i [(z_{0j}^i/x)^9 - (z_{0j}^i/x)^3] & \text{for } x > 0 \\ \infty & \text{otherwise.} \end{cases} \quad (2)$$

Without loss of generality, we assume that the parameters z_{0j}^i are independent of species and wall indices and equal to 0.5σ . The case of the so-called nonselective adsorption [2,17–21,26–28] is met if the energy parameters ε_j^i are identical for both species at both walls. However, in this work we shall study the adsorption between the so-called opposing [4] (or antisymmetric) walls, for which $\varepsilon_1^1 = \varepsilon_2^2 \equiv \varepsilon^{w1}$ and $\varepsilon_1^2 = \varepsilon_2^1 \equiv \varepsilon^{w2}$, i.e., the adsorbing field exerted by the first wall on the molecules of the first component is equal to the field exerted by the second wall on the particles of the second component, and vice versa.

The fluid particles interact via a truncated Lennard-Jones potential

$$u_{jl}(r) = \begin{cases} \varepsilon_{jl} [(\sigma/r)^{12} - (\sigma/r)^6] & \text{for } r < r_{cut} \\ 0 & \text{otherwise,} \end{cases} \quad (3)$$

where $r_{cut} = 2.5\sigma$ is the cutoff distance. The use of a cutoff in theoretical calculations is not necessary. The reason for its introduction is to facilitate a comparison of theoretical predictions with future computer simulation results.

The energy parameter of the Lennard-Jones potential between unlike particles, $\varepsilon_{12}/\varepsilon$, has been assumed to be equal to 0.75. Hereafter we use σ and ε as the units of length and energy, respectively. Similarly, we define the reduced temperature as $T^* = kT/\varepsilon$.

The local densities $\rho_i(\mathbf{r})$ of both species ($i=1,2$) are computed according to a density functional approach. In the present study we use the theory originally derived by Rosenfeld [15,16]. Because this theory has been described and used in several papers, see, e.g., Refs. [17–21], we present the final equations only.

The density profile equation, obtained by minimizing the excess grand canonical potential,

$$\begin{aligned} \Delta\Omega &= \Phi[\rho_1(\mathbf{r}), \rho_2(\mathbf{r})] - \Phi[\rho_{b1}, \rho_{b2}] \\ &- \sum_{i=1}^2 \int d\mathbf{r} \{ \mu_i [\rho_i(\mathbf{r}) - \rho_{bi}] - \rho_i(\mathbf{r}) v_i(\mathbf{r}) \} \\ &+ \sum_{i=1}^2 \int d\mathbf{r} \{ [\rho_i(\mathbf{r}) \ln \rho_i(\mathbf{r}) - \rho_i(\mathbf{r})] - [\rho_{bi} \ln \rho_{bi} - \rho_{bi}] \} \\ &+ \frac{1}{2} \sum_{i,j=1}^2 \int d\mathbf{r} \int d\mathbf{r}' [\rho_j(\mathbf{r}') \rho_i(\mathbf{r}) - \rho_{bj} \rho_{bi}] u_{ij}^{(att)}(|\mathbf{r} - \mathbf{r}'|) \end{aligned} \quad (4)$$

reads

$$\begin{aligned} \ln[\rho_i(\mathbf{r})/\rho_{bi}] &= -\frac{1}{kT} \sum_{a=0}^3 \int \left\{ \frac{\partial \Phi}{\partial n_a(\mathbf{r}')} - \left(\frac{\partial \Phi}{\partial n_a} \right)_{\{\rho(\mathbf{r}')=\rho_{bi}\}} \right\} w_a \\ &\times (|\mathbf{r} - \mathbf{r}'|) d\mathbf{r}' - \frac{1}{kT} \sum_{a=1}^2 \int \left\{ \frac{\partial \Phi}{\partial n_{va}(\mathbf{r}')} \right\} \mathbf{w}_{va} \\ &\times (|\mathbf{r} - \mathbf{r}'|) d\mathbf{r}' - v_i(\mathbf{r})/kT \\ &+ \sum_{j=1}^2 \int d\mathbf{r}' [\rho_j(\mathbf{r}') - \rho_{bj}] u_{ij}^{(att)}(|\mathbf{r} - \mathbf{r}'|). \end{aligned} \quad (5)$$

In the above, μ_i is the configurational chemical potential of the component i , ρ_{bi} is the bulk density of the i th component, Φ is the free energy functional of hard spheres [15,16],

$$\begin{aligned} \Phi/kT &= -n_0 \ln(1 - n_3) + \frac{n_1 n_2 - \mathbf{n}_{v1} \cdot \mathbf{n}_{v2}}{(1 - n_3)} \\ &- \frac{n_2}{24\pi} \frac{[n_2^2 - \mathbf{n}_{v2} \cdot \mathbf{n}_{v2}]}{(1 - n_3)^2}, \end{aligned} \quad (6)$$

and the quantities n_a and \mathbf{n}_{va} are the averaged densities, given by the following equations:

$$n_a(r_1) = \sum_{i=1}^2 \int d\mathbf{r}_2 \rho_i(\mathbf{r}_2) w_a(r_{12}), \quad a=0,1,2,3 \quad (7a)$$

and

$$\mathbf{n}_{va}(\mathbf{r}_1) = \sum_{i=1}^2 \int d\mathbf{r}_2 \rho_i(\mathbf{r}_1 + \mathbf{r}_2) \mathbf{w}_{va}(\mathbf{r}_2), \quad a=1,2, \quad (7b)$$

where $w_a(r, \sigma)$, $a=0,1,2,3$ (scalar quantities), and $\mathbf{w}_{va}(\mathbf{r})$, $a=1,2$ (vector quantities), are the weight functions, chosen such that the Percus-Yevick equation is recovered for a homogeneous fluid. It is worth mentioning that the vectorial contribution to the free energy for a homogeneous fluid is zero. The weight functions are given in Ref. [15]. Moreover, $u_{ij}^{(att)}(r)$ denotes the attractive part of the Lennard-Jones potential (1), defined, as common, according to the Weeks-Chandler-Andersen scheme [34],

$$u_{ij}^{(att)}(r) = \begin{cases} -\varepsilon_{ij}, & r < r_{ij,\min} \\ u_{ij}(r), & r \geq r_{ij,r\min}, \end{cases} \quad (8)$$

where $r_{ij,\min} = 2^{1/6}\sigma$.

The relationship between μ_i and ρ_{bi} is

$$\begin{aligned} \mu_i/kT &= -\ln(1 - n_3) + (\sigma/2)n_2/(1 - n_3) + (\sigma/2)^2 \{ n_1/(1 - n_3) \\ &+ (1/8\pi)n_2^2/[(1 - n_3)^2] \} \\ &+ (\sigma/2)^3 [n_0/(1 - n_3) + n_1 n_2/(1 - n_3)^2 + (1/12\pi)n_3^2/(1 - n_3)^3] \\ &+ \sum_{j=1,2} \rho_{bj} \int d\mathbf{r} u_{ij}^{(att)}(r), \end{aligned} \quad (9)$$

where the average densities are calculated according to Eq. (7a) with local densities equal to the bulk densities. We also introduce the symbol x to abbreviate the bulk fluid composi-

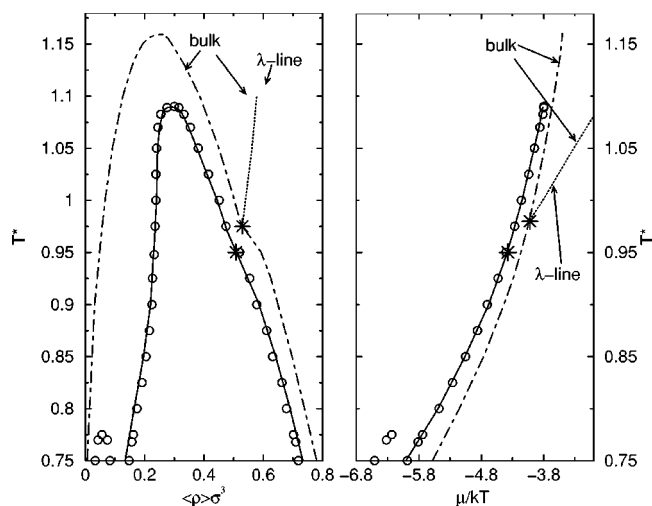


FIG. 1. The capillary condensation in the pore of $H=10\sigma$ with identical walls $\varepsilon^{w1}=\varepsilon^{w2}=11\varepsilon$ (solid lines) and with antisymmetric walls $\varepsilon^{w1}=11\varepsilon$ and $\varepsilon^{w2}=0.01\varepsilon$ walls (open circles). The left panel gives the average density-temperature envelope and the right panel the configurational chemical potential-temperature diagram. In both panels stars denote the locus of the critical end point. We have also included the bulk phase diagrams. The bulk λ lines are denoted by dotted lines.

tion, $x=\rho_{b1}/\rho_b$, where $\rho_b=\rho_{b1}+\rho_{b2}$ is the total bulk fluid density.

The knowledge of the density profiles allows us to calculate the adsorption isotherms of each species, Γ_i ,

$$\Gamma_j = \int_0^H dz [\rho_j(z) - \rho_{bj}]. \quad (10)$$

The total adsorption isotherm Γ is a sum of individual adsorptions, $\Gamma=\Gamma_1$ and Γ_2 . We also define the average fluid density in the pore as $\langle \rho \rangle = \Gamma/H$ and its composition (selectivity) as $S=\Gamma_1/\Gamma$.

The methods used to solve the density profile equations, as well as to evaluate the phase diagrams, have been described in our previous works [17–21].

III. Results and Discussion

We investigate adsorption from a gas phase (i.e., the bulk gas densities are always lower than the bulk dew point density), at an equimolar, $x=0.5$, composition. Therefore the configurational chemical potentials of both species are identical, and for this reason we drop the species indices.

We begin with a brief outline of the phase diagram of the bulk fluid, which for several models has been evaluated earlier and presented in our recent works [17–21]. The diagram for the fluid in question is displayed in Fig. 1. This plot has been prepared assuming that the gas-phase composition is kept constant and equal to $x=0.5$. The bulk critical temperature is equal to $T_{b,c}^* \approx 1.16$ and the λ line, which characterizes demixing, approaches the liquid branch of the gas-liquid envelope at the critical end point temperature. The critical end point temperature is lower than the critical temperature

$T_{b,CEP}^* \approx 0.98$. At the temperatures below $T_{b,CEP}^*$ the liquid condenses into a demixed fluid, whereas at temperatures higher than $T_{b,CEP}^*$ both phases are mixed and characterized by $x=0.5$.

In order to demonstrate how the differences in the adsorbing properties of the two pore walls influence the phase behavior of a confined fluid, we have performed calculations for several pores characterized by a fixed value of the parameter $\varepsilon^{w1}=11\varepsilon$ and varying the value of ε^{w2} .

The above value of the parameter ε^{w1} has been selected to avoid the appearance of layering transitions in the case of a pore with identical walls at the reduced temperatures higher than ≈ 0.75 , and to assure that the pore walls are wet within the investigated range of temperatures. In other words, our intention has been to avoid perturbations connected with the occurrence of layerings and with possible changes in the wettability of the pore walls. Majority of our calculations has been carried out for the pore of the width $H=10\sigma$.

We have started our study with the evaluation of the phase diagrams for the fluid confined in a pore with identical walls, $\varepsilon^{w1}=\varepsilon^{w2}=11\varepsilon$, and in the pore in which each of the species is preferentially adsorbed only by one wall. Setting $\varepsilon^{w1}=11\varepsilon$ and $\varepsilon^{w2}=0.01\varepsilon$ we model the situation in which the particles of the first component are accumulated at the wall, located at $z=0$, whereas the particles of the second component are accumulated at the wall placed at $z=H$. The reason for which we have not used simply opposing hard walls is that we just want to have comparable volumes accessible to adsorbate molecules in all investigated cases. For this reason, the application of a soft (but almost completely) repulsive potential seems to be a better choice.

Figure 1 shows the phase diagrams, evaluated for the two above described model pores, as well as the corresponding bulk phase diagram. Solid lines denote the results for the pore with identical walls. Because we are interested in the phenomenon of capillary condensation only, the relevant plot of the λ line for confined systems has been omitted, and only the critical end point temperature has been marked by a star. Obviously, both the critical and the critical end point temperatures are lower than the corresponding bulk values. At the temperatures lower (higher) than the critical end point temperature the capillary condensation leads to a demixed (mixed) adsorbed liquid.

The shape of the capillary condensation part of the phase diagram evaluated for opposing walls is very close to the situation with identical walls, cf. dashed lines in Fig. 1. Note that the critical capillary condensation temperatures are almost identical in those two systems. The similarity of both phase diagrams does not imply that thermodynamic properties of those systems are also very similar. In particular, the shape of adsorption isotherms (see Fig. 2) for the pores with opposing and identical walls are different. In the former case the adsorption isotherm exhibits a rounded step at low chemical potentials, being a reminiscence of the first layering transition, which has been found at still lower temperatures.

The opposing walls enforce the layering, and at the lowest investigated temperatures we observe the occurrence of the envelope associated with the layering transition within the layers adjacent to the pore walls. This effect is quite similar to that observed for single-component fluids [13,14]. The

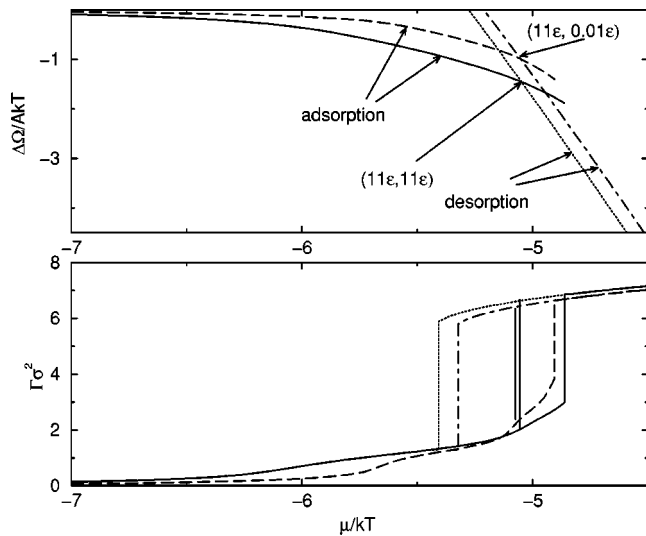


FIG. 2. Examples of the plots of the excess grand potentials (upper panel) and of the isotherms (lower panel) for the systems with identical walls and with antisymmetric walls. The nomenclature of the lines is explained in the upper panel. Here the numbers in parentheses denote the values of ϵ^{w1} and ϵ^{w2} and the lines labeled adsorption and desorption denote adsorption and desorption branches. Vertical solid lines in the lower panel indicate the equilibrium transitions. The calculations have been carried out for $H = 10\sigma$ and at $T^* = 0.85$.

occurrence of the layering is the first qualitative difference in the thermodynamic behavior of the two systems in question. Another difference between the systems with identical and with opposing walls concerns the lack of the critical end point temperature and the demixing inside the pore in the latter case. The composition of a fluid confined in the pore with $\epsilon^{w1} = 11\epsilon$ and $\epsilon^{w2} = 0.01\epsilon$ is always equal to $S = 0.5$. This can be understood by inspection of the local densities. The density profile for both components (see Fig. 3) are perfectly antisymmetric, so that the density profile of one component can be obtained by reflecting the profile for the second component with respect to the line $z = H/2$. Therefore, we shall call such a confined fluid structure as antisymmetric. Obviously, the symmetry of the confined fluid follows from the symmetry of the external potential field. Both confined systems, before and after capillary condensation, are antisymmetric.

The capillary condensation leads to a development of a kind of an “interface” at the pore center, separating “1-rich” from “2-rich” films. The development of such an interface costs extra work (cf. the plot of $\Delta\Omega$ in Fig. 2). The price for that work can be paid if the difference in the adsorbing potential between two walls with respect to both components, i.e., the difference $|\epsilon^{w1} - \epsilon^{w2}|$ is big enough. However, if this difference is small, different pore filling scenarios are possible and the rest of our work is devoted to the discussion of such situations.

We now consider the case in which the difference $|\epsilon^{w1} - \epsilon^{w2}|$ is small. In Fig. 4 we show thermodynamic properties characterizing capillary condensation in the case when $\epsilon^{w1} = 11\epsilon$ and $\epsilon^{w2} = 10\epsilon$ at $T^* = 0.85$. Left, central, and right panels display the excess grand potential, adsorption isotherm, and

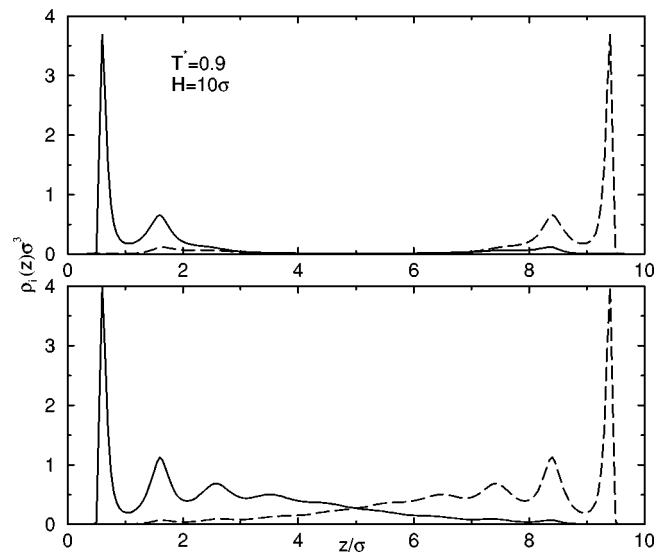


FIG. 3. Examples of the density profiles of two species (solid and dashed lines) before (upper panel) and after (lower panel) capillary condensation transition in the pore with antisymmetric walls, $\epsilon^{w1} = 11\epsilon$ and $\epsilon^{w2} = 0.01\epsilon$ at $T^* = 0.9$. The pore width is $H = 10\sigma$.

and the selectivity versus the configurational chemical potential, respectively. Dotted lines correspond to adsorption of rarefied phase, whereas solid and dashed lines correspond to the adsorption of dense, liquidlike phases. If the bulk gas density increases from zero (or if the configurational chemical potential increases from minus infinity) to the value corresponding to the point labeled 1 in Fig. 4, the following

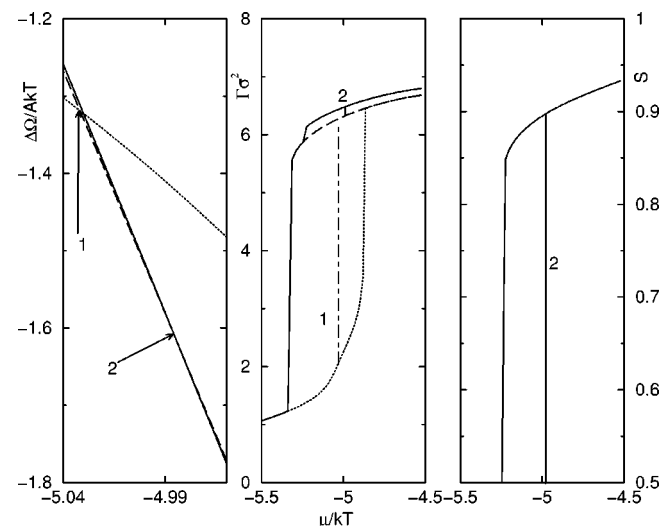


FIG. 4. The plot of the excess grand potential (left panel), of the adsorption isotherm (central panel), and of the selectivity (right panel). The calculations have been carried out for $\epsilon^{w1} = 11\epsilon$ and $\epsilon^{w2} = 10\epsilon$, $H = 10\sigma$, and at $T^* = 0.85$. Dotted lines correspond to (antisymmetric) gaslike phase, dashed lines to antisymmetric liquidlike phase, and solid lines to a demixed liquidlike phase. Labels 1 and 2 denote the capillary condensation and the antisymmetric film-demixed film transition, respectively. Vertical, dash-dotted line, with label 1, and solid line, with label 2, indicate equilibrium transitions.

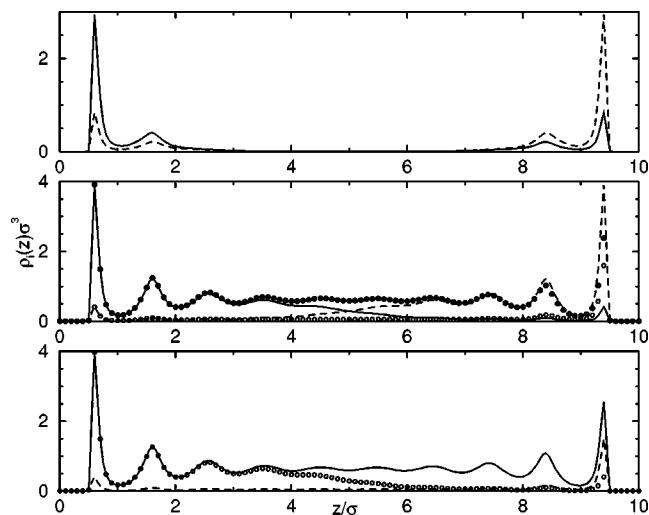


FIG. 5. Changes in the structure of the confined fluid during phase transitions shown in Fig. 4. Solid and dashed lines are for thermodynamically stable states, whereas open and closed circles denote metastable states. Upper panel displays the density profiles of rarefied phase at point 1 in the phase diagram in Fig. 3. Middle panel shows stable and metastable density profiles of the liquidlike adsorbed phase at point 1, whereas lower panel shows the profiles after the antisymmetric film–demixed film transition at point 2. Here only one profile for the metastable state is displayed. The profile for the second component is symmetric with respect to the pore center. The values of all parameters are the same as in Fig. 4.

changes occur. At very low bulk gas densities the density profiles are close to the ideal gas distributions, i.e., antisymmetric films start to develop. With an increasing bulk gas density the density profiles change and directly before the capillary condensation transition we observe the existence of two adlayers at each pore wall. Capillary condensation occurs at the chemical potential corresponding to point 1. This process leads to the formation of antisymmetric, liquidlike film inside the pore, cf. upper panel of Fig. 5. However, already at that value of the configurational chemical potential there exists an additional solution to the density profile equation (7a) and (7b). This solution is marked by dots in the middle panel of Fig. 5 and corresponds to a demixed film, without an interface at the pore center. We abbreviate that kind of film as a demixed one. However, this film (the thermodynamic quantities characterizing that film are marked by solid lines in Fig. 4) is metastable with respect to antisymmetric film—the latter corresponds to lower value of the grand potential, cf. left panel of Fig. 4. At the point labeled by 2 the situation changes, namely, the antisymmetric film becomes metastable with respect to the demixed film, cf. lower panel in Fig. 5. It is an abrupt process, which is accompanied by a jump at the adsorption isotherm (the corresponding branches of the excess grand potential do intercept) and therefore it occurs as a first-order transition, cf. central panel in Fig. 4.

A discontinuous demixing is the main difference, compared with the case of pores with identical walls. The demixing observed inside the pore with identical walls “beyond” the first-order capillary condensation transition has been of the second order [17–21].

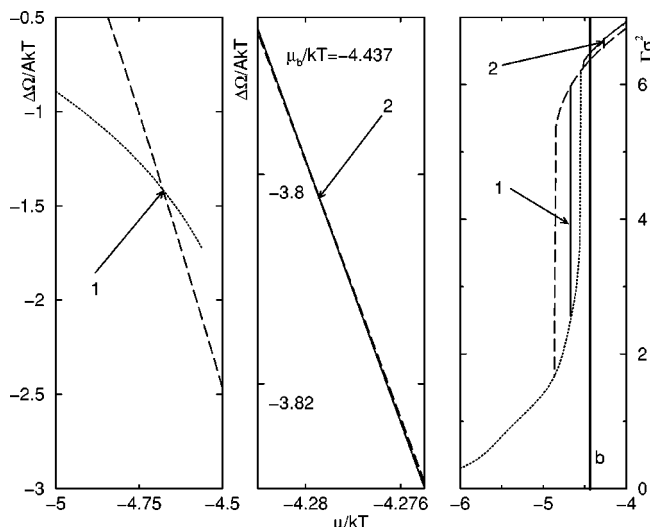


FIG. 6. The plot of the excess grand potential (left and central panels) and of the adsorption isotherm (right panel). The calculations have been carried out for $\epsilon^{w1}=11\epsilon$ and $\epsilon^{w2}=10\epsilon$, $H=10\sigma$, and at $T^*=0.9$. Dotted lines correspond to (antisymmetric) gaslike phase, dashed lines to antisymmetric liquidlike phase, and solid lines to a demixed liquidlike phase. Labels 1 and 2 denote the capillary condensation and the antisymmetric film–demixed film transition, respectively. Vertical, dash-dotted line, with label 1, and solid line, with label 2, indicate equilibrium transitions. For a better visualization of the transitions, the plots of the grand potential for capillary condensation and for the antisymmetric-demixed film transition have been plotted in two distinct panels. The value of the chemical potential at the bulk dew point is given in the central panel and the thick vertical line, labeled *b* indicates the locus of the bulk gas–fluid transition.

With the temperature increase (see Fig. 6) up to $T^*=0.9$ the following changes occur. The condensation at point 1 leads to antisymmetric film and there is still a possibility to obtain solutions corresponding to demixed films, but this transition occurs at the chemical potential above the value corresponding to the bulk gas–liquid transition. Thus, we can conclude that if the adsorption takes place from a gaseous bulk phase the antisymmetric-demixed film transition observed in Fig. 4 ends at the temperature at which the chemical potential becomes equal to the chemical potential at the bulk coexistence. For the system in question this temperature is $T_2^*\approx 0.88$. We stress that above the temperature T_2^* the antisymmetric-demixed film transition can still be found, but at bulk densities higher than the bulk dew density.

In contrast, when the temperature decreases, the picture of the pore filling becomes different. Figure 7 is an analog of Fig. 4. The data presented here have been evaluated at $T^*=0.75$. The value of ϵ^{w2} has been also changed and equals now 9.5ϵ . Under such conditions the capillary condensation leads directly to a demixed film and antisymmetric liquidlike film is always metastable with respect to a demixed film. In other words there exists some characteristic temperature T_1^* , below which the capillary condensation leads to a demixed film. Note that the adsorption branch of the isotherm in Fig. 7 shows a sequence of layerings (to make them more visible the dotted line in the central panel of Fig. 7 has been deco-

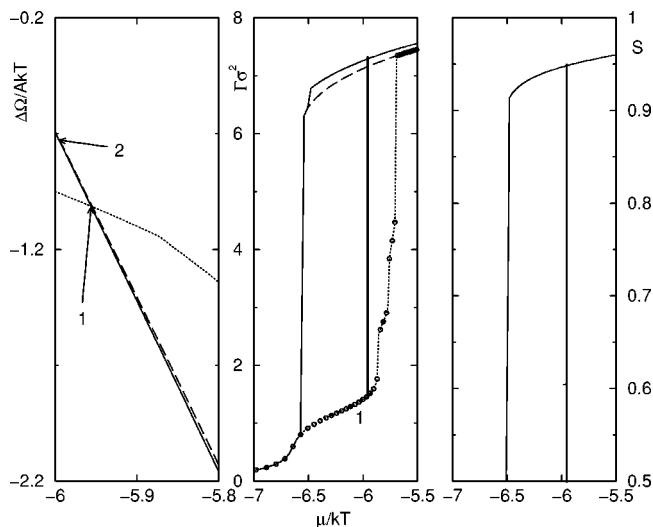


FIG. 7. The same as in Fig. 4, but for $\varepsilon^{w1}=11\varepsilon$ and $\varepsilon^{w2}=9.5\varepsilon$, $H=10\sigma$, and at $T^*=0.75$. To make metastable (with respect to the capillary condensation) layerings more visible the dotted line in the central panel has been decorated with points.

rated with points), but they are metastable with respect to the capillary condensation, which takes place at point 1.

The results presented so far indicate that there exist the following possible scenarios of capillary condensation.

Below some characteristic triple point temperature T_1^* , the capillary condensation leads to a demixed film in the entire pore, without an interface at the pore center.

At the temperature higher than T_1^* the condensation leads to an antisymmetric film. However, there may also exist a second first-order transition between antisymmetric and demixed films. Taking into account the experimental conditions, i.e., the fact that in our “experimental setup” the adsorption occurs from gaseous phase, we can also distinguish the temperature T_2^* as the temperature at which the antisymmetric-demixed film transition occurs at the chemical potential equal to the chemical potential at the bulk gas-liquid coexistence. Obviously, T_2^* is not a threshold for different pore filling mechanism, but it characterizes the crossing between the pore filling mechanism and the bulk condensation.

A different behavior has been found if the difference between ε^{w1} and ε^{w2} is large enough. In such systems the condensed liquidlike phase is always antisymmetric—thus, presumably the temperature T_1^* drops to zero. This is also the reason for which we do not observe demixing transition on the phase diagram in Fig. 1 for the fluid adsorbed in the pore with opposing walls.

If the difference in the adsorbing potential between two walls decreases to zero, the first-order antisymmetric-demixed film transition reduces to the λ line. One can thus expect for a nonzero difference $|\varepsilon^{w1}-\varepsilon^{w2}|$ the first-order antisymmetric-demixed transition must terminate at the critical end point temperature, at which the first-order transition transforms into the λ line.

Figure 8 presents the phase diagram for the system with $\varepsilon^{w1}=11\varepsilon$ and $\varepsilon^{w2}=10\varepsilon$ in the density-temperature (left panel) and the chemical potential-temperature (right panel)

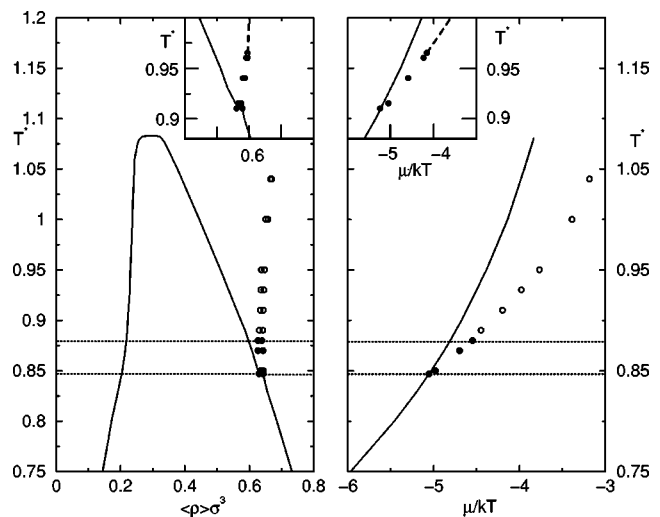


FIG. 8. Phase diagram for the system with $\varepsilon^{w1}=11\varepsilon$ and $\varepsilon^{w2}=10\varepsilon$, $H=10\sigma$ in the average density-temperature plane (left panel) and in the configurational chemical potential-temperature plane (right panel). Lines denote capillary condensation envelope, points correspond to the antisymmetric film-demixed film transition. Lower and upper horizontal dotted lines denote the triple point temperature T_1^* and the temperature T_2^* , respectively. Insets to both panels show parts of the phase diagrams, obtained for $\varepsilon^{w1}=11\varepsilon$ and $\varepsilon^{w2}=10.6\varepsilon$. In this case the antisymmetric-demixed first-order transition ends at the critical end point. The λ line, being its continuation, is marked as thick dotted line.

planes, respectively. Lower horizontal dotted line denotes the triple point temperature T_1^* and the upper dotted line denotes the temperature T_2^* . Filled and open circles represent the first-order transition between antisymmetric and demixed liquid-like films. To distinguish adsorption from gas and liquid phases the transition points have been marked with open circles in Fig. 8. We stress that the capillary condensation critical temperature for the present system is nearly the same as for the systems plotted in Fig. 1.

For the system with $\varepsilon^{w1}=11\varepsilon$ and $\varepsilon^{w2}=10\varepsilon$ the reduced critical end point temperature is higher than 1.04. The value of the critical end point temperature decreases with a decrease of the difference $|\varepsilon^{w1}-\varepsilon^{w2}|$. We have carried out additional calculations for the system with $\varepsilon^{w1}=11\varepsilon$ and $\varepsilon^{w2}=10.6\varepsilon$. The results are displayed in the insets to left and right panels of Fig. 8. In this case the estimated value of the critical end point temperature is $T^* \approx 0.96$ and is nearly equal to the temperature T_2^* .

For a fixed value of ε^{w1} a decrease of ε^{w2} lowers those temperatures, whereas an increase of the pore width shifts T_1^* towards higher values. In Fig. 9 we have displayed the dependence of T_1^* on the energy ε^{w2} and on the pore width. The value of ε^{w1} was fixed and equal 11ε . If the value of ε^{w2} is low enough, layering transitions may appear. In this work, however, we have not explored the situations in which layering transitions occur and, therefore, we have not studied a possible competition between layerings and capillary condensation. On the other hand, when the value of ε^{w2} approaches ε^{w1} (i.e., 11ε in our case), the temperature T_1^* approaches the critical end point temperature of the system

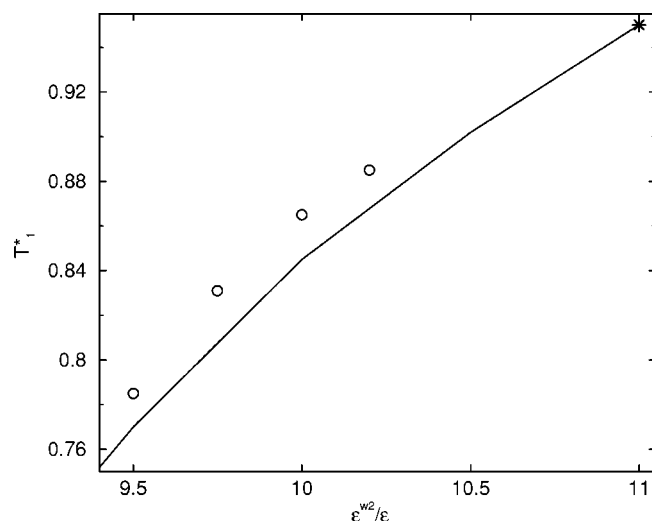


FIG. 9. Dependence of the triple point temperature T_1^* on ϵ^{w2} for $H=10\sigma$ (line) and for $H=20\sigma$ (points). The value of ϵ^{w1} is 11ϵ . The star indicates the critical end point temperature for the system with $\epsilon^{w1} = \epsilon^{w2} = 11\epsilon$.

with identical walls and the entire envelope of the antisymmetric-demixed film transition meets the λ line.

Let us summarize briefly our work. In the case of adsorption in slitlike pores with antisymmetric walls a new pore filling scenario has been found. It takes place when the difference between the strength of the adsorbing potentials at both walls is small enough and the temperature is lower than the characteristic triple point temperature T_1^* . Under such

conditions, the capillary condensation transition leads to the formation of a demixed film. The symmetry properties of that demixed film do not follow the symmetry of the appropriate Boltzmann factors. At the temperatures higher than T_1^* , the capillary condensation leads to antisymmetric films, which exhibit the same symmetry as the symmetry of the external fields acting on both components. A further increase of the bulk density enforces the occurrence of the second first-order transition between the antisymmetric and demixed films. This first-order transition ends at its critical end point temperature, above which it transforms into λ line.

There are several problems, which still need to be solved. In particular, we have not investigated the effects due to wettability changes in the system and the influence of layering-type transitions on the phase behavior of a binary mixture in pores with antisymmetric walls. Next, we have investigated only one bulk fluid model, with rather high value of the cross energy. It would be of interest to explore other bulk fluid models, e.g., models exhibiting the existence of the tricritical temperatures [35]. Finally, investigation of adsorption in much wider pores, in which it might be possible to find the interface delocalization transition [4] would be also of interest. All these problems are currently under study in our laboratories.

ACKNOWLEDGMENTS

This work was partially supported by the CONACyT of Mexico under Grant No. 37323-E, by UNAM under Grant No. IN-113201, and by KBN of Poland under Grant No. 4T09A15824.

-
- [1] M. Schoen, in *Computational Methods in Surface and Colloid Science*, edited by M. Borówko (Marcel Dekker, New York, 2000).
 - [2] S. Dietrich, in *New Approaches to Problems in Liquid State Theory*, edited by C. Caccamo *et al.* (Kluwer Academic, Amsterdam, 1999), pp. 197–244.
 - [3] L. D. Gelb, K. E. Gubbins, R. Radhakrishnan, and M. Śliwiska-Bartkowiak, *Rep. Prog. Phys.* **62**, 1572 (1999).
 - [4] K. Binder, D. Landau, and M. Müller, *J. Stat. Phys.* **110**, 1411 (2003).
 - [5] K. Binder and E. Luiten, *Phys. Rep.* **344**, 179 (2001).
 - [6] M. Müller, K. Binder, and E. V. Albano, *Physica A* **279**, 188 (2000).
 - [7] A. M. Ferrenberg, D. P. Landau, and K. Binder, *Phys. Rev. E* **58**, 3353 (1998).
 - [8] E. V. Albano, K. Binder, and W. Paul, *J. Phys.: Condens. Matter* **12**, 2701 (2000).
 - [9] M. Müller, K. Binder, and E. V. Albano, *J. Mol. Liq.* **92**, 41 (2001).
 - [10] M. Müller and K. Binder, *Phys. Rev. E* **63**, 021602 (2001).
 - [11] K. Binder, M. Müller, and E. V. Albano, *Phys. Chem. Chem. Phys.* **3**, 1160 (2001).
 - [12] E. Carlon and A. Drzewiński, *Phys. Rev. E* **57**, 2626 (1998).
 - [13] R. Zagórski and S. Sokołowski, *J. Colloid Interface Sci.* **240**, 219 (2001).
 - [14] R. Zagórski, A. Patrykiewicz, and S. Sokołowski, *J. Phys.: Condens. Matter* **14**, 165 (2002).
 - [15] Y. Rosenfeld, *Phys. Rev. Lett.* **63**, 980 (1989).
 - [16] J. A. Cuesta, Y. Martinez-Raton, and P. Tarazona, *J. Phys.: Condens. Matter* **14**, 11 965 (2002).
 - [17] K. Bucior, A. Patrykiewicz, S. Sokołowski, and O. Pizio, *J. Colloid Interface Sci.* **259**, 209 (2003).
 - [18] K. Bucior, A. Partykiewicz, O. Pizo, S. Sokołowski, and Z. Sokołowska, *Mol. Phys.* **101**, 721 (2003).
 - [19] A. Martinez, O. Pizio, and S. Sokołowski, *J. Chem. Phys.* **118**, 6008 (2003).
 - [20] A. Martinez, A. Patrykiewicz, O. Pizio, and S. Sokłowski, *J. Phys.: Condens. Matter* **15**, 3107 (2003).
 - [21] K. Bucior, *Colloids Surf., A* **219**, 113 (203).
 - [22] F. Bulnes, A. J. Ramirez-Pastor, and V. D. Pereyra, *J. Mol. Catal. A: Chem.* **167**, 129 (2001).
 - [23] W. T. Gózz, K. E. Gubbins, and A. Z. Panagiotopoulos, *Mol. Phys.* **84**, 825 (1995).
 - [24] Z. Tan and K. E. Gubbins, *J. Phys. Chem.* **96**, 845 (1992).
 - [25] E. Schöll-Paschinger, D. Levesque, J.-J. Weis, and G. Kahl, *Phys. Rev. E* **64**, 011502 (2001).
 - [26] E. Paschinger and G. Kahl, *Phys. Rev. E* **61**, 5330 (2000).
 - [27] L. Tremblay, S. M. Socol, and S. Lacelle, *Phys. Rev. E* **61**,

- 656 (2000).
- [28] G. Kahl, E. Schöll-Paschinger, and A. Lang, *Monatsch. Chem.* **132**, 1413 (2001).
- [29] J. Reszko-Zygmunt, A. Patrykiewicz, S. Sokołowski, and Z. Sokołowska *Mol. Phys.* **100**, 1905 (2002).
- [30] P. A. Gordon and E. D. Glandt, *J. Chem. Phys.* **105**, 4257 (1996).
- [31] S. Iatsevitch and F. Forstmann, *J. Phys.: Condens. Matter* **13**, 4769 (2001).
- [32] M. Wendland, *Fluid Phase Equilib.* **147**, 105 (1998).
- [33] J. Stecki and S. Toxvaerd, *J. Chem. Phys.* **102**, 7163 (1995); **103**, 4352 (1995); **103**, 9763 (1995).
- [34] J. D. Weeks, D. Chandler, and H. C. Andersen, *J. Chem. Phys.* **54**, 5237 (1971).
- [35] N. B. Wilding, F. Schmid, and P. Nielaba, *Phys. Rev. E* **58**, 2201 (1998).